NRIAG JOURNAL OF ASTRONOMY AND GEOPHYSICS
2020, VOL. 9, NO. 1, 483–490
https://doi.org/10.1080/20909977.2020.1773741

Structural setup of Gara Marine area as deduced from 3D seismic interpretation and gravity-magnetic modelling, Gulf of Suez, Egypt

A. Ghoneimi[a], A. Azab[b], M. Elsawy[b] and A. Alaa El-Din[b]

[a]Geology Department, Faculty of Science, Zagazig University, Zagazig, Egypt; [b]Exploration Department, Egyptian Petroleum Research Institute, Cairo, Egypt

ABSTRACT

An integrated interpretation utilising seismic data and inverse modelling is executed to more-reveal the subsurface complexity in Gara Marine area. The shallow features are identified by doing the seismic analyses on tops of Miocene formations. The deeper structures are deduced through constructing two gravity-magnetic models constrained by seismic and well data. The seismic results indicate that upper-Miocene rocks are characterised by a thick salt section (~2Km), which rarely cut by faults. South Gharib exhibits a structural closure at the centre due to a salt dome with dipping limbs towards the east and west. Belayim and Kareem are thinner in thickness, uniform distribution and steeply dipping to the southwest. Rudeis seems thicker westward, deposited in the downthrown side of a master block-fault. The uncertainty in seismic interpretation due to Miocene salts is estimated on tops of different horizons (±70 m static). The models indicate that Pre-Miocene sediments were deposited on a rough basement surface, with southwest regional dip-regime. The basement is deformed by the cross-faults (NW and NE) which vanish within Miocene section, with no evidences support presence of magmatic materials. The dip-reversal along flanks of Miocene salt structure, and limbs of pre-Miocene uplift, are the most potential traps.

ARTICLE HISTORY
Received 18 February 2020
Revised 17 May 2020
Accepted 20 May 2020

KEYWORDS
Gulf of Suez; Egypt; Gara Marine; seismic interpretation; applied geophysics

1. Introduction

Deep seismic imaging in the Gulf of Suez area is extremely problematic due to the serious effect of the near-surface thick evaporites. The major difficulty is encountered in defining and imaging of the pre-Miocene horizons where the interpretation becomes quite poor due to (1) thick Miocene evaporite section which is responsible for the attenuation and absorption of seismic energy. (2) Multiple events/reflections that came from the post-Miocene and Miocene evaporites, which masked the weak reflections from the pre-Miocene interfaces. (3) Dip reversals observed in the Miocene strata, which have different dips in all directions, affected the data acquired, and velocity analysis interpretation. (4) Large thickness of Rudeis clastics that reaches in some parts to one thousand metres, causing absorption and scattering of both the down going and reflected energies. (5) Closed space faults caused a lot of diffraction and scattered noises, which may be interfered and stacked giving pseudo reflections of indefinite trends (Meshref et al. 1976; Nakhla 2005; Zahra and Nakhla 2016). All of these reasons may cause a lack of penetration of the seismic energy, with little or no energy/waves reach the ground surface (Cao and Brewer 2013).

Actually, it is found that the 2D seismic data interpretation is limited by the base of Miocene evaporites, where the deepest reliable interface is Kareem–Rudeis. To overcome the seismic failure an integrated interpretation using potential field data, seismic reflection and well data were carried out through applying the inverse modelling technique. The deep source structures in the area could be identified by constructing two joint gravity-magnetic models. In order to reduce the ambiguity of potential field data, the shallow portion of the models was constrained by the seismic lines, geologic information and well data. The actual densities, thicknesses and depths of the Miocene formations have been well defined, which reduce ambiguity and help deduce the pre-Miocene source structures through iterative fitting between the calculated and observed profiles.

The study aims to define the shallow structural features intervening the Gara Marine area depending on the seismic line package (Figure 1) and well data, to obtain improved images on tops of Miocene formations. Then, establishing combined gravity-magnetic models, constrained by seismic sections and well information, to a better understanding of the pre-Miocene source structures including; uplifts and basins, basement composition, igneous intrusions, fault-linkages above and below the basement surface.

The material used in the study area is composed of a grid of 29 SEG-Y format 2D seismic reflection lines derived from a 3D seismic data volume. These lines

CONTACT A. Alaa El-Din www.ahmedalaaeldin93@hotmail.com

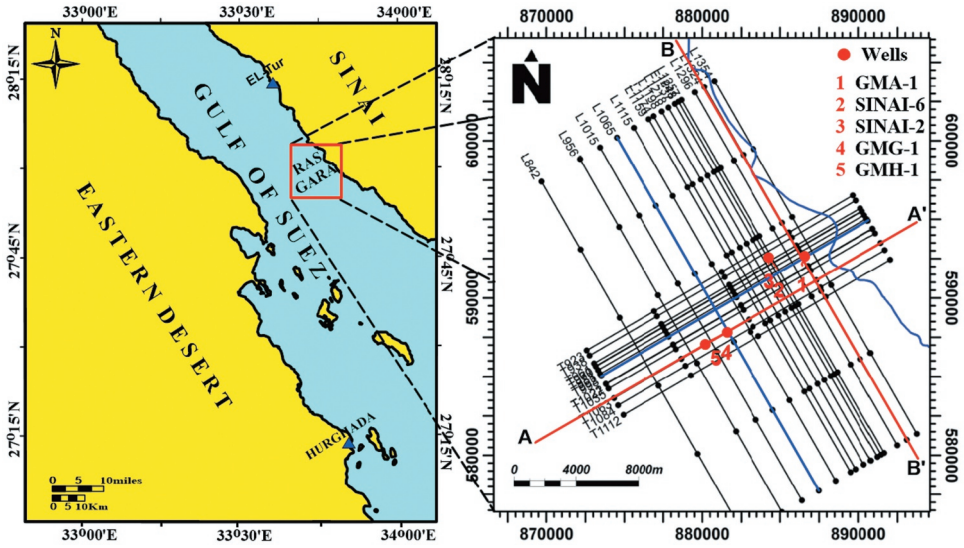

Figure 1. Location map of Ras Gara area showing shot points locations, modelled profiles (red) along seismic crossline T1063 (A–A′) and inline L1324 (B–B′), and interpreted seismic sections (blue) L1065 and T998.

are classified into 15 NW-SE oriented inlines and 14 NE-SW oriented crosslines. The time–depth relations (check-shots) of five wells are used to detect the marker horizons of Miocene age. In addition, the potential field data include both of (1) Bouguer gravity anomaly map with scale 1:100,000, and contour interval of 1 mGal, which had been measured by General Petroleum Company (GPC) in 1976. (2) Total intensity aeromagnetic survey map of southern Gulf of Suez (Ras Gara concession), with a scale of 1:250,000, and contour interval of 5 Gammas, which had been surveyed and compiled by GPC in 1986, for Egyptian General Petroleum Corporation (EGPC).

2. Geologic setting

The Gara Marine area is a part of Ras Gara concession which is located in the offshore portion of the southern province of the Gulf of Suez (Figure 1). It is situated some 30 km to the south of El Tor City, between latitudes 27°56′10″N and 28°03′38″N and longitudes 33°38′41″E and 33°50′54″E, and covers about 100 km^2. The stratigraphic succession of the Gara Marine oil field (Figure 2(a)) is characterised by a thick Miocene section (Nukhul, Rudeis, Kareem, Belayim, South Gharib and Zeit Formations). The pre-Miocene section (Nubia, Matulla, Sudr, Esna and Thebes Formations) is characterised by the reduced thickness (about 550 m) unconformably overlain by the Miocene clastics and evaporite sequences (>2500 m) which in turn overlain by sediments of the Post-Zeit Formation. The Miocene oil reservoirs are mainly represented by upper-Rudeis and Kareem Formations which are characterised by lateral facies variations, while the pre-Miocene oil reservoir is essentially represented by Matulla Formation (Salama et al. 1994). The hydrocarbon implications indicate that the exploration activity started in 1964 with Gara Marine-1 well, a Miocene oil discovery. Several wells were drilled until 1987 when Sinai oil field (Miocene and pre-Miocene oil) was discovered. This field is the only commercial discovery in Ras Gara area, which is currently on production with an average rate of 12,000 BOPD. Fifteen wells were drilled in Ras Gara concession, since 1964 until 1994 (Salama et al. 1994), producing hydrocarbons from the lower-middle Miocene reservoirs. The hydrocarbon traps dominating in and around the area of investigation are of structural and combined types. The middle/upper Miocene evaporate rocks represent a main seal or hydrocarbon traps for the Early-Middle Miocene, as well as pre-Miocene reservoirs. The structural-tectonic framework of the southern Gulf of Suez (Figure 2(b)) was discussed recently by many authors (e.g. Patton et al. 1994; Sharp et al. 2000; Rohais et al. 2016; Bosworth and Durocher 2017; Segev et al. 2017; Temraz and Dypvik 2018).

3. Methodology

This study starts with the 2D seismic data interpretation to define the structural elements on tops of the sedimentary formations. The structural interpretation depends mainly on twenty-nine 2D offshore seismic lines divided into fifteen in-lines trends in strike direction and fourteen cross-lines in dip direction, in addition to check-shots of five boreholes classified into four directional wells (GMA-1, GMH-1, SINAI-2 and SINAI-6) and one vertical well (GMG-1). Depending on Petrel Software, the ordinary steps of seismic interpretation was carried out which include; seismic-to-well tie to find the seismic reflectors that coincide with the formations tops by using check-shot data of boreholes and synthetic seismograms, to trace upper Miocene (Zeit and South Gharib), Middle Miocene (Belayim

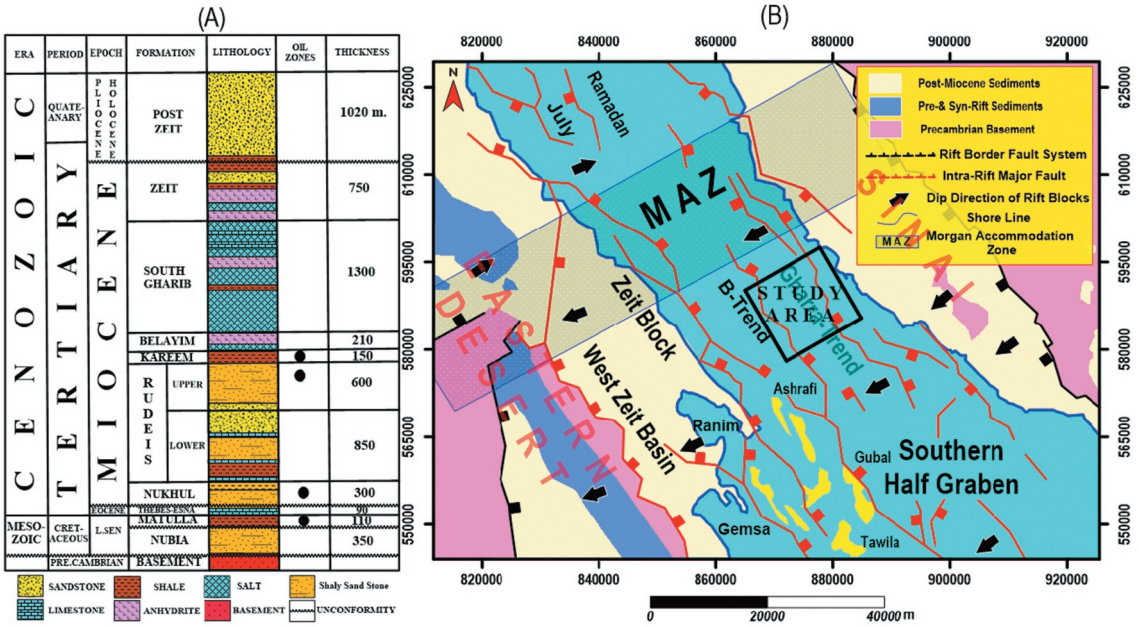

Figure 2. (a) Schematic stratigraphic column of Ras Gara area (after Salama et al. 1994) and (b) Tectonic map of the southern portion of the Gulf of Suez (after Patton et al. 1994).

and Karem) and lower Miocene (Rudeis) horizons at SEG-Y format time-migrated seismic sections. Picking horizons separating different rock layers, fault detection with a large displacement of rocks. Construction of two-way time (TWT) maps, velocity mapping using five wells, time to depth conversion, depth structural mapping and thickness mapping.

Thereafter, an integrated approach has been implemented utilising the inverse modelling to give an improved image of the blind seismic zone below the evaporites. Two joint gravity-magnetic models were constructed along two interpreted seismic sections (inline and crossline) in two different (strike and dip) directions. The models are constrained by well data and geologic information to confirm the shallow structures, and to help deduce the deep source bodies.

4. 2D seismic interpretation

The 2D seismic interpretation is applied for five selected seismic markers (from Zeit to Rudeis) on the seismic lines (Figure 1), tied with five drilled wells (GMA-1, GMH-1, GMG-1, SINAI-2, SINAI-6). Figure 3 shows two examples of the relations between time versus depth and velocities of GMA-1 and GMG-1 wells. The interval velocity is variable according to lithology, reaches maxima against the Belayim Formation (anhydrite) while noticeably decreases against Kareem and Rudeis Formations (clastics). Figure 4(a) shows that the time-migrated cross-line (NE-dip oriented line) is of the best quality and reasonably reliable. The seismic reflectors have a good quality in Zeit and South Gharib Formations, fairly good in Belayim, Kareem and Rudeis Formations, and uncertain or bad quality in the deeper horizons beneath the base of Rudeis Formation. The Gara Marine structure, at Miocene level, is a SW-dipping block, bounded from the west by a major block-fault (F1) of first-order magnitude, with a large vertical displacement to east forming deep basin. The depth to the formations decreases eastward at the upthrown side of the tilt-block, while increases westward at the downthrown side of the master fault (F1). The thick salt formations (Zeit and South Gharib) are distinguished by a dome-like feature, with a steep dip of limbs, which are rarely fractured by faults. Whereas the sub-salt formations (Belayim, Kareem, Rudeis) are fractured by the Clysmic faults that increase in the number and length with depth. The seismic events on the in-line (Figure 4 (b)) could be ranked between poor to fair. The structure at Miocene level reflects a gentle regional dip regime to the southeast, with a slight increase in thickness of the sedimentary layers. This structure is characterised by lack of faults along this trend; with no evidence support presence of traverse faults deform Miocene formations.

5. Uncertainty of interpretation

Well data matching with the seismic events (Table 1) showed that the seismic sections are deeper/shallower from the actual one, with about ±70 m static shift. This uncertainty is essentially back to the velocity difference and complex geometry of the Miocene salts. The uncertainty is critical if the velocities of the salts and the overload are not similar, so that moving the

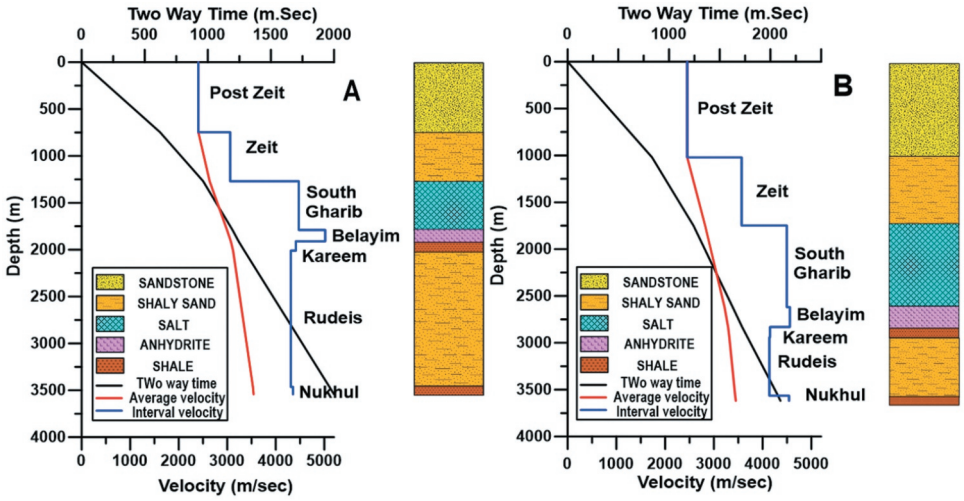

Figure 3. Time and velocity versus depth of (a) GMA-1 well and (b) GMG-1 well.

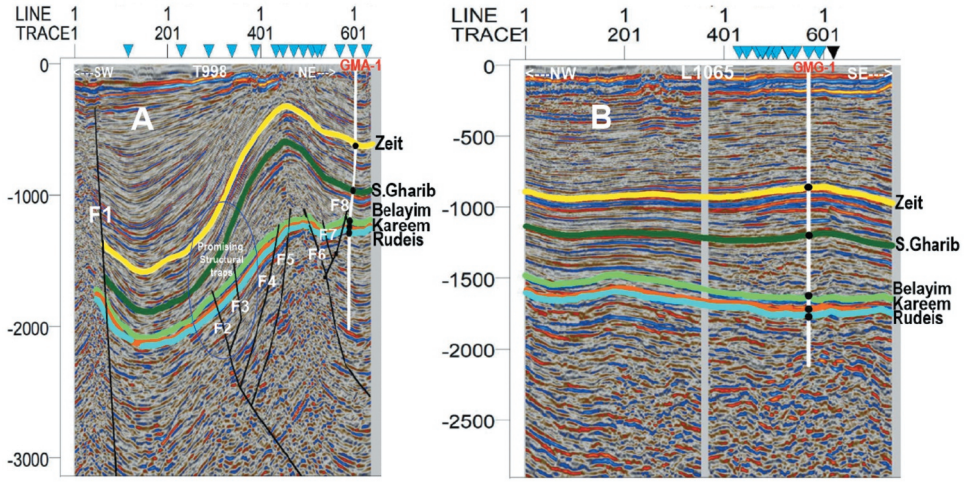

Figure 4. Interpreted seismic lines showing the picked horizons and structural elements. (a) Cross-line T998 (SW-NE) and (b) In-line L1065 (NW-SE).

contact up or down will make a little difference to the deeper image. If the salt layer (South Gharib) has a faster velocity than the surrounding formations, the P-waves travelling through the salt layer return to receivers more quickly, creating the velocity pull-up. Whereas if the salt layer is slower than the surroundings, the P-waves travelling through the salt return to receivers more slowly, producing the velocity push-down. Actually, the Miocene evaporite rocks are not pure halite (seismic velocity Vp ~4500 m/s), but contain significant amounts of gypsum (Vp ~5700 m/s), anhydrite (Vp ~6500 m/s) and K-Mg-rich salts (Vp ~3500 m/s). The heterogeneity and variable salt composition, as well as other factors such as water–gas, water–oil interfaces greatly affect the speed; causing the salt velocity pull-up or push-down. Also, the rapid changes in the thickness of salt cause problems for mapping the actual configurations of the underlying formations. Practically with time migration, the reflection from beds, due to the salt structure, is poorly defined because of the algorithm is unable to correctly handle distortion of ray-paths passing through the thick salt (~2000 m) of the Zeit and South Gharib Formations and anhydrite section of Belayim Formation.

6. Depth structural mapping

The time maps of different horizons are converted into depth maps using the average velocity grid of all wells in the area. Generally, the resultant depth-structure maps (Figure 5) show similar distributions where the depth increases generally towards the west and decrease to the east. The structural-depth contour map on top of Zeit Formation (Figure 5(a)) exhibits a large depth value (−1500 m) in the western side and a small depth value (−500 m) in the east. Westward, the map demonstrates a major NW-trending block-fault (F1) of first-order magnitude, with a large throw to the east. The depth-structure map on top of South

Table 1. Depth uncertainty through available wells.

Well name	Depth (m) (Estimated)	Depth (m) (Actual)	Difference	Difference%	Formation
SINAI-6	570	563.05	6.95	1.23	**Z e l t**
SINAI-2	580	569.99	10.01	1.76	
GMA-1	745	746.72	−1.72	−0.23	
GMH-1	1210	1186.76	23.24	1.96	
GMG-1	1095	1021	74	7.25	
SINAI-6	1070	1070.17	−0.17	−0.02	**S. Gharib**
SINAI-2	1050	1068.1	−18.1	−1.69	
GMA-1	1270	1270.03	−0.03	0.00	
GMH-1	2450	2458.62	−8.62	−0.35	
GMG-1	1740	1749	−9	−0.51	
SINAI-6	1900	1908.76	−8.76	−0.46	**Belayim**
SINAI-2	1790	1797.29	−7.29	−0.41	
GMA-1	1780	1790.15	−10.15	−0.57	
GMH-1	2830	2765.65	64.35	2.33	
GMG-1	2650	2619	31	1.18	
SINAI-6	1950	1951.54	−1.54	−0.08	**Kareem**
SINAI-2	1870	1914.78	−44.78	−2.34	
GMA-1	1900	1910.58	−10.58	−0.55	
GMH-1	2960	2954.17	5.83	0.20	
GMG-1	2830	2831	−1	−0.04	
SINAI-6	2030	2045.38	−15.38	−0.75	**Rudeis**
SINAI-2	1940	1947.78	−7.78	−0.40	
GMA-1	1960	2009.87	−49.87	−2.48	
GMH-1	3010	3051.9	−41.9	−1.37	
GMG-1	2940	2940	0	0.00	

Gharib Formation (Figure 5(b)) exhibits a similar structural pattern with a large depth ranges from −1000 to −3000 m. The depth-structure maps on tops of middle-lower Miocene formations (Figure 5 (c–e)) show a comparable distribution of depths. Eastward, the maps exhibit seven normal faults (F2-F8) below the salt structure, with different throws, are running parallel to each other in the NNW-SSE direction (Clysmic trend). The depth of top Belayim (Figure 5(c)) varies from −2000 to −3000 m, top of Kareem (Figure 5(d)) ranges between −2000 and −3500 m and top Rudeis (Figure 5(e)) is from −2000 to −3500 m.

7. Thickness (isopach) maps

A set of seismic isopach maps is established to reflect the variations in the thickness of the stratigraphic rock units of Miocene age (from Zeit to Rudeis), which are characterised by a large thickness variation from east to west. The isopach map of Zeit Formation (Figure 6(a)) displays a large thickness in the western side that reaches 1500 m, while the small thickness attains 500 m in the eastern part. Conversely, the isopach map of South Gharib Formation (Figure 6(b)) shows a rapid increase in thickness of the salts towards the east. The thickness reaches a maximum of 1000 m correlated with the domal feature, while the minimum is 500 m. The pre-salt formations (Belayim, Kareem, Rudeis) are generally characterised by lesser thicknesses, with uniform shape and SW regional dip regime. The isopach map of Belayim Formation (Figure 6(c)) shows a small thickness ranges between 200 and 50 m, of Kareem Formation (Figure 6(d)) varied from 120 to 20 m, while Rudeis Formation (Figure 6(e)) is from 500 to 1500 m.

8. Inverse modelling

The RTP map (Figure 7(a)) and Bouguer anomaly map (Figure 7(b)) were used to deduce the deep structures/sources of the lower portion of the sedimentary section utilising the inverse modelling technique. Two combined gravity-magnetic models were constructed in both dip and strike directions, constrained by seismic lines and well data. The models focus attention on the uppermost portion of the earth's crust with a depth of 6 km. The sedimentary cover was modelled as 2D layers, with assuming homogenous formations. The geometry of the shallow rock units (Miocene strata) was constrained by the seismic sections, and their parameters (density and depth) were controlled by the borehole data. The deeper portion (pre-Miocene and basement) of the model could be deduced through obtaining a reasonable fit between the observed and calculated anomalies. The gravity-magnetic matching was iteratively estimated until the best fit has reached.

The first model (Figure 8(a)) is constructed along profile A–A$^{\backslash}$(Figure 7), extends in the NE-SW trend (dip direction). The upper portion of the sedimentary cover was constrained by the seismic cross-line T1063 and two drilled wells (GMH-1 and GMG-1). The Gara Marine area is composed of several tilted fault-blocks, with a regional dip regime to the southwest. The upper-Miocene salts (Zeit and South Gharib formations) are characterised by a thick section, particularly towards the centre, with little or no deformation. The thickness of the post-Miocene sediments increases outward away from the anticlinal salt structure. The Middle Miocene sediments (Kareem and Belayim Formations) are

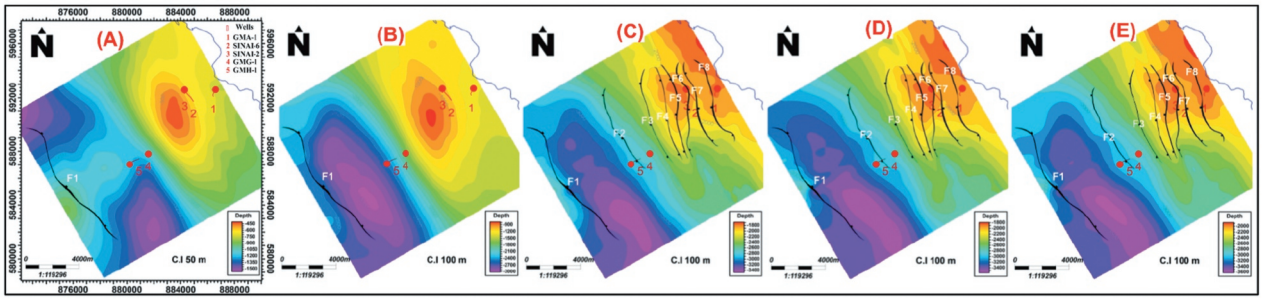

Figure 5. Depth-structuree maps of tops (a) Zeit, (b) South Gharib, (c) Belayim, (d) Kareem and (e) Rudeis.

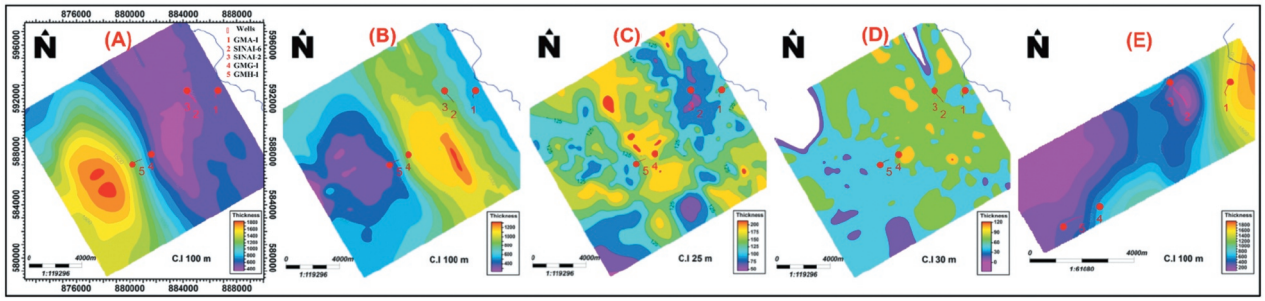

Figure 6. Thickness (isopach) maps of (a) Zeit, (b) South Gharib, (c) Belayim, (d) Kareem and (e) Rudeis.

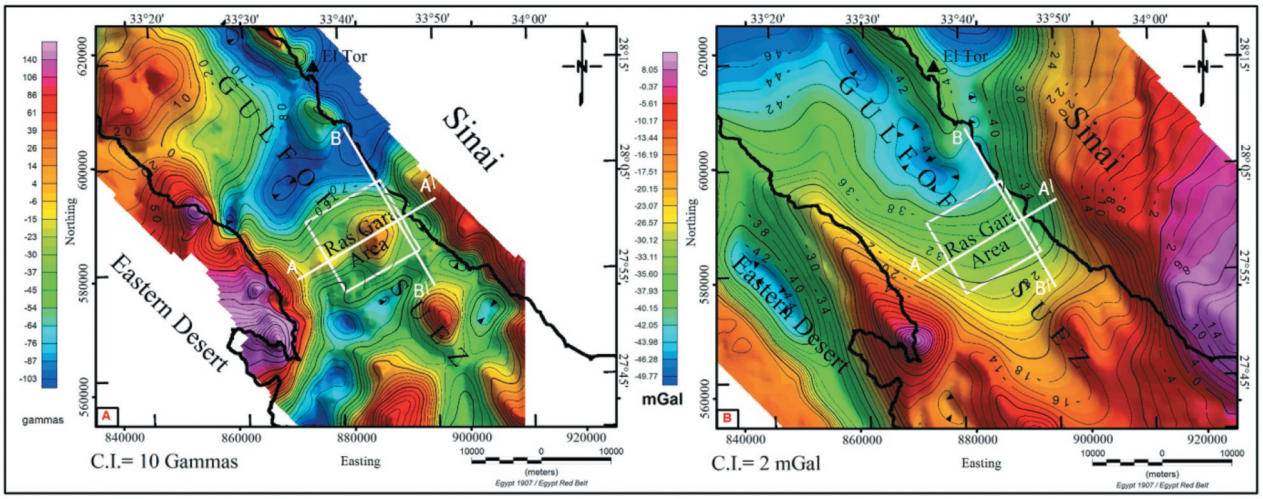

Figure 7. Potential field data (a) RTP magnetic map, (b) Bouguer anomaly map, with locations of modelling profiles.

nearly of uniform thicknesses, sloping down to the west. The model shows that the pre-Miocene sediments have deposited on a rough basement surface, with depth variation ranges from 1.5 to 5 km. The pre-salt structure exhibits a large number of the NW-trending faults (Clysmic trend), of different slopes and throws, which divided the area into sub-blocks of different sizes and tilts. The majority of these faults arisen on basement surface, rejuvenated into the overlying pre-Miocene sequence, and vanished into the Miocene/subsalt formations. Magnetically, the Gara Marine is an anomalous feature in the central area, which is correlated with uplifted basement blocks (P7, P8). The normal susceptibility values give no evidence support presence of any igneous intrusions along this trend.

The second model (Figure 8(b)) is constructed along profile B–B\'(Figure 7) parallel to the Gulf of Suez, in the NW-SE direction (strike direction). The geometry of the shallow sedimentary layers (Miocene formations) was seismically controlled by Inline L1324 and tied with GMA-1 well. Generally, the post-Miocene and Miocene strata are fairly running smooth, dipping gently to the northwest, and seem to be not entirely deformed by major faults (Aqaba trend). The deeper portion or seismically blind zone of pre-Miocene seems to be thicker towards the west, with no evidence support presence of faults. The basement relief is generally dipping gently towards the northwest, associated with low gravity-magnetic responses. The basement surface is disturbed by a number of cross-gulf faults (NE-SW faults) of different tilts and low magnitude of throws. The basement blocks show normal susceptibility (0.0001–.0.005 cgs-unit) and density (2.6–2.7 g/cm3) with no magmatic penetration. Tables 2 and 3 summarized the parameters deduced from gravity-magnetic models and seismic.

9. Discussion

The quality of seismic data seems good at the Miocene level whilst blind below the Miocene evaporite where no consistent seismic reflection can be safely recorded. This is logic since the evaporite group is thick and characterised by thin layers of anhydrite, salt, marl and gypsum with intercalated streaks of sandstone, creating high reflection coefficients at each change in lithology. These interfaces generate internal multiples and seismic energy attenuation, which are very destructive.

The seismic interpretation on tops of Miocene formations shows a good relation to the NW-SE Gulf of

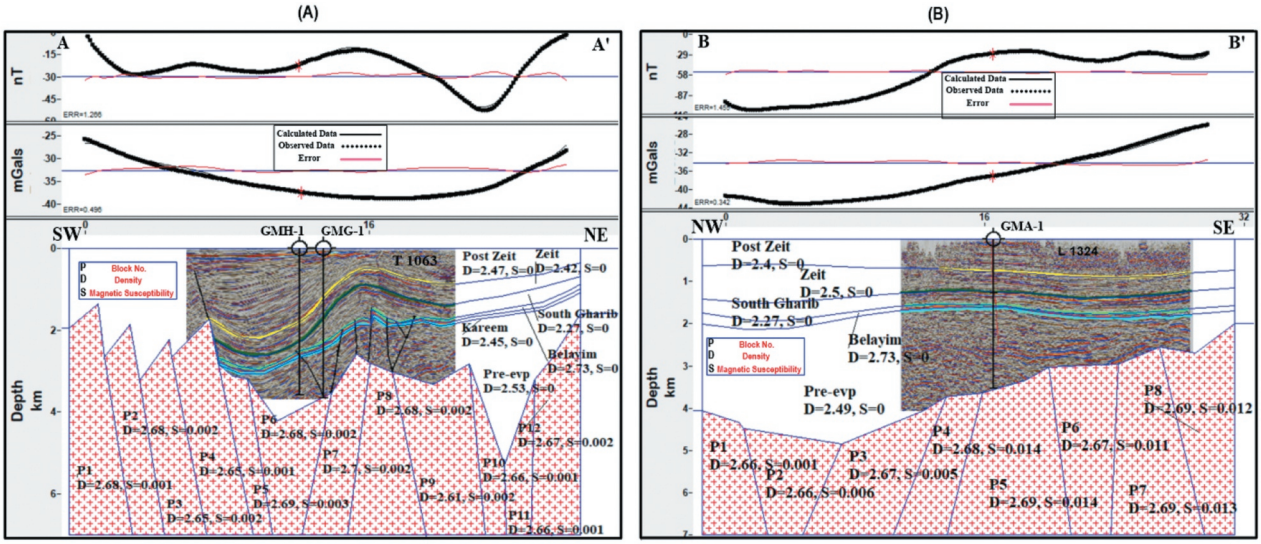

Figure 8. Gravity-magnetic modelling along dip direction (A–A′) and strike direction (B–B′).

Table 2. Gravity, magnetic and seismic parameters deduced from model A–A′.

Tops of		Density (gm/cc)	Mag. suscept. (cgs)	Depth range (km)
Sedimentary layers	Post-Zeit	2.47	0	0
	Zeit	2.42	0	0.51–2.22
	S. Gharib	2.27	0	0.89–2.6
	Belayim	2.73	0	1.6–2.94
	Kareem	2.45	0	1.66–3.01
	Pre-evp	2.53	0	1.75–3.08
Basement blocks	P1	2.68	0.0013	~1.66
	P2	2.68	0.0016	~2.3
	P3	2.65	0.0014	~2.71
	P4	2.65	0.0008	~2.2
	P5	2.69	0.0025	~3.12
	P6	2.68	0.0023	~4.23
	P7	2.7	0.0015	~2.62
	P8	2.68	0.0016	~2.93
	P9	2.61	0.0023	~3.35
	P10	2.66	0.0011	~3.98
	P11	2.66	0.0012	~4.14
	P12	2.67	0.0019	~2.36

Table 3. Gravity, magnetic and seismic parameters deduced from model B–B′.

Tops of		Density (gm/cc)	Mag.sus-cept. (cgs)	Depth range (km)
Sedimentary layers	Post-Zeit	2.4	0	0
	Zeit	2.5	0	0.69–0.91
	S.Gharib	2.27	0	1.21–1.42
	Belayim	2.73	0	1.57–1.77
	Pre-evp	2.49	0	1.63–1.9
Basement blocks	P1	2.66	0.0006	~4.06
	P2	2.66	0.0055	~4.66
	P3	2.67	0.004	~4.39
	P4	2.68	0.0137	~3.71
	P5	2.69	0.0139	~3.48
	P6	2.67	0.011	~3.01
	P7	2.69	0.0134	~2.76
	P8	2.69	0.0115	~2.62

Suez trend, while no relation with the NE-SW Aqaba trend. This may be back to the fact that the transform faults have geometries which make difficult to see them on seismic sections (Meshref 1990). The NE-trending faults are characterised by large horizontal displacements and relatively small magnitude of throws (Garson and Krs 1976).

The structure interpreted at pre-Miocene level confirms that the cross gulf-faults (Aqaba trend), which are rare in seismic maps, seem to be abundant on the basement surface. This may indicate that both of the NW-SE and NE-SW trending faults are of deep-seated origin (Meshref et al. 1976), and thought to be a pre-rift structural fabric (Garfunkel and Bartov 1977). They seem to be inherited from old fractures and developed preferentially along pre-existing lines of weakness on the basement surface (Moustafa 1976).

Seismic interpretation indicates the presence of a salt closure at top of upper-Miocene South Gharib Formation. It is also believed that such salt diapiric feature may have formed along zones of weakness due to differential isostatic load of the thick post-Miocene sediments.

The uncertainty in picking base and top of the salt formations (South Gharib, Zeit) cause problems for mapping the actual configurations of the Miocene rock units. Wells data matching with the seismic events showed that the seismic reflectors are deeper/shallower from the actual ones. The anomalous seismic velocities of the salt rocks and their complex geometry create a large complexity in the seismic wave paths, causing the velocity difference above/below the thick salt section. This is logic since the inhomogeneous salt composition, and variation in thickness of salt, as well as other factors such as laminations and water–gas, water–oil interfaces are causing the velocity pull-up and/or push-down.

The central part of the Gara marine area is considered to be of large priority and focal point in any further

explorations. The anticlinal structure due to pre-Miocene uplift and Miocene domal feature (salt structure) represents structural traps for the surrounding basins. The steep limbs provide a high possibility of entrapment of the hydrocarbons from the low topographic areas.

10. Conclusions

The integrated seismic interpretation and gravity-magnetic modelling show that Gara Marine oilfield is situated on a NE-SW tilted fault-block with a westward regional dip regime. The inner structure is complicated by a set of Clysmic faults at different levels that start on basement surface, rejuvenated into the overlying pre-Miocene section and die out into the Miocene strata. The NE-trending faults seem less prominent at Miocene level but are very abundant on the basement surface and play a main role in complicating the area. The joint models suggest homogeneous basement rocks, overlain by a heterogeneous sedimentary cover, with no evidence support presence of any igneous intrusions.

The results suggest that the central portion is the most suitable for entrapment and accumulation of hydrocarbons. The pre-Miocene structure has greatly affected by basement uplift which causes dip-reversal on both sides, whereas the Miocene salts have largely influenced by a domal feature with steeply dipping flanks, the western limb is the most promising structural traps.

Disclosure statement

No potential conflict of interest was reported by the authors.

ORCID

A. Ghoneimi http://orcid.org/0000-0002-9189-397X
A. Azab http://orcid.org/0000-0002-8652-1610
A. Alaa El-Din http://orcid.org/0000-0002-4085-310X

References

Bosworth W, Durocher S. 2017. Present-day stress fields of the Gulf of Suez (Egypt) based on exploratory well data: non-uniform regional extension and its relation to inherited structures and local plate motion. J Afr Earth Sci. 136:136–147. doi:10.1016/j.jafrearsci.2017.04.025.

Cao J, Brewer JD. 2013. Critical reflection illumination analysis. Interpret J. 1: T57–T61.

Garfunkel Z, Bartov Y. 1977. The tectonics of the Suez rift. Geol Surv Isr. 71:1–48.

Garson MS, Krs M. 1976. Geophysical and geological evidence of the relationship of Red Sea transverse tectonics to ancient fractures. Geological Society of America Bulletin. 87(2):169–181. doi:10.1130/0016-7606(1976)87<169:GAGEOT>2.0.CO;2.

Meshref W. 1990. Tectonic framework of global tectonics, Geology of Egypt. Netherlands: Balkema/Ratterdam/Bookfield; p. 439–449.

Meshref W, Refai EM, Abdel Baki SM. 1976. Structural interpretation of the Gulf of Suez and its oil potentialities. Proceedings of the 5th Explor. Semin., E. G.P.C; November 1976; Egyptian General Petroleum Organization-Deminex, Cairo, Egypt. p. 21.

Moustafa AM. 1976. Block faulting in the Gulf of Suez. Proceedings of the 5th Explor. Semin., E.G.P.C; November 1976; Egyptian General Petroleum Organization-Deminex, Cairo, Egypt. p. 36.

Nakhla AM. 2005. An integrated seismotectonic- magneto-tectonic study for the miocene-pre-miocene sequence in Abu Rudeis-Ras Budran area Gulf of Suez, Egypt [Ph.D. thesis]. Geology department, Banha University.

Patton TL, Moustafa AR, Nelson RA, Abdine AS. 1994. T 100ectonic evolution and structural setting of the Suez rift. In: Landon SM, editor. Interior rift basins. AAPG Memoir. Vol. 59; p. 9–55.

Rohais S, Barrois A, Colletta B, Moretti I. 2016. Pre-salt to salt stratigraphic architecture in a rift basin: insights from a basin-scale study of the Gulf of Suez (Egypt). Arab J Geosci. 9(4):317. doi:10.1007/s12517-016-2327-8.

Salama A, El-Mougy S, El-Moneim MA, Hakim S. 1994. Exploration in Ras Ghara area, a case history, Southern Gulf of Suez, Egypt. Egypt J Pet Corp. 1:240–257.

Segev A, Avni Y, Shahar J, Wald R. 2017. Late Oligocene and Miocene different seaways to the Red Sea–Gulf of Suez rift and the Gulf of Aqaba–Dead Sea basins. Earth-Science Reviews. 171:196–219. doi:10.1016/j.earscirev.2017.05.004.

Sharp IR, Gawthorpe RL, Underhill JR, Gupta S. 2000. Fault-propagation folding in extensional settings: examples of structural style and synrift sedimentary response from the Suez rift, Sinai, Egypt. Geol Soc Am Bull. 112 (12):1877–1899. doi:10.1130/0016-7606(2000)112<1877:FPFIES>2.0.CO;2.

Temraz M, Dypvik H. 2018. The Lower Miocene Nukhul Formation (Gulf of Suez, Egypt): microfacies and reservoir characteristics. J Pet Explor Prod Technol. 8(1):85–98. doi:10.1007/s13202-017-0386-3.

Zahra HS, Nakhla AM. 2016. Structural interpretation of seismic data of Abu Rudeis-Sidri area, Northern Central Gulf of Suez, Egypt. NRIAG J Astron Geophys. 5 (2):435–450. doi:10.1016/j.nrjag.2016.09.002.